are satisfied. In the walking support, HAL stops the sequential walking support and helps a wearer come back to the standing posture when the condition:

$$t_{\text{cur}} - t_{\text{r}} > T_{\text{wait}} \quad \text{or} \tag{9}$$

$$t_{\text{cur}} - t_{\text{l}} > T_{\text{wait}}, \tag{10}$$

is satisfied, where t_{cur}, t_{r} and t_{l} are the current time and the time when the last right or left foot touched the floor. In addition, T_{wait} is a temporal threshold to switch the walking support to the standing posture support. At this moment, the reference angles of all joints are almost zero; therefore, the backward leg is replaced around the forward leg if a load on the backward leg becomes almost zero by his/her weight shift. We set $T_{\text{wait}} = 5.0$ s in this experiment.

4.3. Control architecture

Bipedal locomotion using a patient's legs is achieved by tracking control and by phase synchronization of motion support with the patient's intention. This control consists of the PD control using reference walking patterns based on a healthy person's walk as shown in Fig. 7a in the swing phase and the constant-value control in the landing and support phase. Figure 8 shows a block diagram for this tracking control and phase synchronization. The human intention estimator (HIE) located in the upper-left part in Fig. 8 has the FRF as input for the estimation algorithms described in Section 4.2. Three blocks under the HIE are a library of the reference

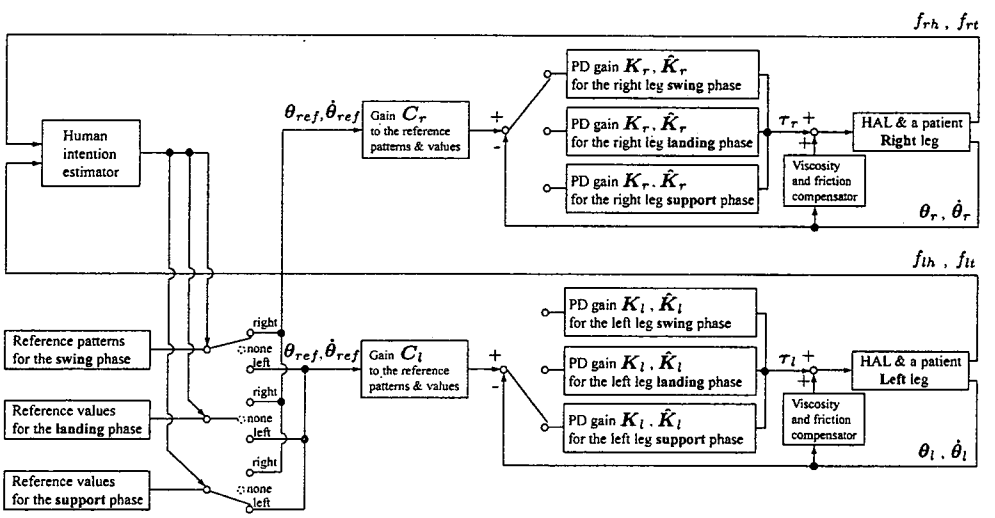

Figure 8. Block diagram for tracking control and phase synchronization. The HIE has the FRF as input for the estimation algorithms described in the previous section. Three blocks under the intention estimator are a library of the reference patterns in three walking phases, and the reference values in the landing and support phase. The intention estimator allocates these references to the two legs during walking. The ordinary PD control blocks are shown on the right side of the intention estimator and the library.

patterns in the swing phase, and the reference values in the landing and support phase. The HIE allocates these references to the two legs during walking. There are six ordinary PD control blocks on the right side of the HIE and the library. The upper three blocks are controllers for the right leg and the lower ones are for the left leg. The command voltages $\boldsymbol{\tau}_r$ and $\boldsymbol{\tau}_l$ to the power units on both legs are calculated by:

$$\boldsymbol{\tau}_r = \mathbf{K}_r(\mathbf{C}_r\boldsymbol{\theta}_{ref} - \boldsymbol{\theta}_r) + \hat{\mathbf{K}}_r(\mathbf{C}_r\dot{\boldsymbol{\theta}}_{ref} - \dot{\boldsymbol{\theta}}_r) \tag{11}$$

and

$$\boldsymbol{\tau}_l = \mathbf{K}_l(\mathbf{C}_l\boldsymbol{\theta}_{ref} - \boldsymbol{\theta}_l) + \hat{\mathbf{K}}_l(\mathbf{C}_l\dot{\boldsymbol{\theta}}_{ref} - \dot{\boldsymbol{\theta}}_l), \tag{12}$$

where $\boldsymbol{\theta}_r$ and $\boldsymbol{\theta}_l$ are the actual wearer's leg joint angles, $\dot{\boldsymbol{\theta}}_r$ and $\dot{\boldsymbol{\theta}}_l$ are angular velocities, and subscripts r and l mean right and left, respectively. In addition, $\boldsymbol{\theta}_{ref}$ and $\dot{\boldsymbol{\theta}}_{ref}$ are the reference joint angles and the reference angular velocities, respectively. These variables including $\boldsymbol{\tau}_r$ and $\boldsymbol{\tau}_l$ have two elements that correspond to two joints: the hip and knee joint. $\boldsymbol{\tau}_r$, $\boldsymbol{\tau}_l$, $\boldsymbol{\theta}_r$, $\boldsymbol{\theta}_l$, $\dot{\boldsymbol{\theta}}_r$, $\dot{\boldsymbol{\theta}}_l$, $\boldsymbol{\theta}_{ref}$ and $\dot{\boldsymbol{\theta}}_{ref}$ are given as follows:

$$\boldsymbol{\tau}_r = \begin{bmatrix} \tau_{rh} \\ \tau_{rk} \end{bmatrix}, \quad \boldsymbol{\tau}_l = \begin{bmatrix} \tau_{lh} \\ \tau_{lk} \end{bmatrix}, \tag{13}$$

$$\boldsymbol{\theta}_r = \begin{bmatrix} \theta_{rh} \\ \theta_{rk} \end{bmatrix}, \quad \boldsymbol{\theta}_l = \begin{bmatrix} \theta_{lh} \\ \theta_{lk} \end{bmatrix}, \quad \dot{\boldsymbol{\theta}}_r = \begin{bmatrix} \dot{\theta}_{rh} \\ \dot{\theta}_{rk} \end{bmatrix}, \quad \dot{\boldsymbol{\theta}}_l = \begin{bmatrix} \dot{\theta}_{lh} \\ \dot{\theta}_{lk} \end{bmatrix}, \tag{14}$$

$$\boldsymbol{\theta}_{ref} = \begin{bmatrix} \theta_{href} \\ \theta_{kref} \end{bmatrix}, \quad \dot{\boldsymbol{\theta}}_{ref} = \begin{bmatrix} \dot{\theta}_{href} \\ \dot{\theta}_{kref} \end{bmatrix}, \tag{15}$$

where subscripts rh, rk, lh and lk mean right hip joint, right knee joint, left hip joint and left knee joint, respectively. On the other hand, $\mathbf{K}_r$ and $\mathbf{K}_l$ are feedback gains of the joint angle errors, and $\hat{\mathbf{K}}_r$ and $\hat{\mathbf{K}}_l$ are feedback gains of the joint angular velocity errors. The different feedback gains are used in the swing, landing or support phase independently by adopting this control architecture. In addition, $\mathbf{C}_r$ and $\mathbf{C}_l$ are gains to the reference joint angles and angular velocities. These gains can adjust a joint flexion and a stride length in a wearer's supported walk. In this experiment, we set $\mathbf{C}_l$ larger than $\mathbf{C}_r$ in order to avoid collisions of the left leg, which has a more severe paralysis, with the floor in the swing phase. $\mathbf{K}_r$, $\mathbf{K}_l$, $\hat{\mathbf{K}}_r$, $\hat{\mathbf{K}}_l$, $\mathbf{C}_r$ and $\mathbf{C}_l$ are diagonal matrices which are given as follows:

$$\begin{aligned} \mathbf{K}_r &= \begin{bmatrix} k_{rh} & 0 \\ 0 & k_{rk} \end{bmatrix}, \quad \mathbf{K}_l = \begin{bmatrix} k_{lh} & 0 \\ 0 & k_{lk} \end{bmatrix}, \\ \hat{\mathbf{K}}_r &= \begin{bmatrix} \hat{k}_{rh} & 0 \\ 0 & \hat{k}_{rk} \end{bmatrix}, \quad \hat{\mathbf{K}}_l = \begin{bmatrix} \hat{k}_{lh} & 0 \\ 0 & \hat{k}_{lk} \end{bmatrix}, \end{aligned} \tag{16}$$

$$\mathbf{C}_r = \begin{bmatrix} c_{rh} & 0 \\ 0 & c_{rk} \end{bmatrix}, \quad \mathbf{C}_l = \begin{bmatrix} c_{lh} & 0 \\ 0 & c_{lk} \end{bmatrix}. \tag{17}$$

Moreover, the PD gains of swing leg control k_{rh}, k_{lh}, $\hat{k}_{rh}$, $\hat{k}_{lh}$, k_{rk}, k_{lk}, $\hat{k}_{rk}$ and $\hat{k}_{lk}$ were determined based on frequency responses and step responses of the hip and knee joints. The procedure is described in the Appendix.

The control flow for the walking support is as follows. At first, HAL supports a wearer's standing posture. Once the conditions shown in (5) and (6) are satisfied, HAL starts the PD control for the swing phase in the right leg and for the support phase in the left leg. On the other hand, HAL starts the PD control for the swing phase in the left leg and the support phase in the right leg once the conditions shown in (7) and (8) are satisfied. The PD control for a swing leg continues until HAL finishes the reference swing patterns. After that, HAL runs the constant-value control for the landing phase until the condition shown in (1) or (2) is satisfied in a case of the right leg and until the condition shown in (3) or (4) is satisfied in a case of the left leg. The other leg continues the control for the support phase. After HAL detects a contact between the foot of the swing leg and the floor, HAL runs the constant-value control for the support phase on both legs and continues the control until the next swing start conditions are satisfied. If the conditions are not satisfied, the two legs are kept at the final posture of the step. However, the reference angles of all joints are almost zero in this phase, therefore a backward leg is replaced around a forward leg if the load on the backward leg becomes almost zero by his/her weight shift. Thus, a wearer can come back to the standing posture. This algorithm can synchronize walking support with human intentions at a walk start instance, a walk stop instance as well as at the beginning of leg swing during walking. In addition to the walking support, HAL compensates for viscosity and static friction of the power units [3].

5. EXPERIMENT

The participant A is a 57-year-old male SCI patient who has incomplete sensory and motor paralysis on the left leg, especially on the left lower thigh. He is diagnosed with an incomplete SCI; the sixth and seventh thoracic vertebra (T6 and T7) are damaged. While he has good voluntary control of the upper body and limited voluntary control of both legs, he has little voluntary control of the muscles below the left knee joint. His deep sensibility, including angle sensitivity, remains partially intact in his lower thigh; however, tactile, pain and temperature sensitivities are lost. Normally, he can walk quite slowly with limping by using two canes with both his hands. During walking, however, he always feels anxious that his knee joint will suddenly and involuntarily bend during sustaining his weight as a support leg, his leg will not swing forward due to involuntary control of hip and knee flexor muscles, and he will stumble or fall down due to collisions of his 'drop foot' with the floor or the other side support leg during swinging a leg. He has trouble lifting his own leg against gravity, since he experiences significant difficulty climbing up stairs. In addition, he has stiffening of his left knee joint and sometimes spasticity of his left lower thigh muscles. He participated in our experiments more than 3 years after

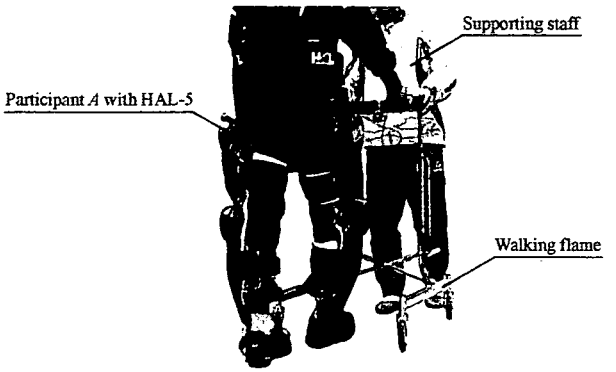

Figure 9. Experimental setting.

sustaining a SCI as a result of a traffic accident. During his admission to hospital, he received regular physical therapy for about 6 months. However, he stopped it after he left the hospital because he could not recognize any improvement in his body functions.

He gave informed consent before participating. All procedures were approved by the Institutional Review Board and the experiments were conducted under the inspection of physical therapists. The aim of HAL support is to help his leg swing forward without a limp and sustain his weight (65 kg) since he can stand with two canes by himself. This support contributes to stabilizing his walk by pushing the swing leg forward, by avoiding collisions of the swing leg with the floor and by preventing sudden knee bends. In this experiment, he walked a straight line in one direction on the flat and non-slippy floor in the laboratory. This walking support was conducted 16 times, and he was required to start walking from a standing posture and stop walking at his own convenience. In each trial, he walked 5–7 m using 12–18 steps. Moreover, he was supposed to maintain his own stability by holding a walking frame with his arms and a staff supports the walking frame for the sake of patient's safety as shown in Fig. 9, since he experienced walking support embedded with the proposed intention estimation algorithm for the first time.

5.1. Experimental setup

In this experiment, the thresholds to detect the moment when the foot leaves the floor or contacts on the floor expressed as α_{rh}, α_{rt}, α_{lh}, α_{lt}, β_{rh}, β_{rt}, β_{lh} and β_{lt} are finally set to 50 N based on the participant's weight and his impression after some trials. On the other hand, the feedback gains for the joint control k_{rh}, k_{lh}, $\hat{k}_{rh}$, $\hat{k}_{lh}$, k_{rk}, k_{lk}, $\hat{k}_{rk}$ and $\hat{k}_{lk}$, the gains to the reference joint angle and velocity errors c_{rh}, c_{rk}, c_{lh}, and c_{lk} and a time span for swinging the leg are adjusted through some trials reflecting the participant's impression. The time span for swinging a leg is finally set to 0.9 s.

5.2. Results

Figures 10 and 11 show the FRF data and phase transitions on each leg during walking support. In both figures, one leg performs as the support leg up to a 'Toe off' moment when (6) or (8) is satisfied, and then the leg performs as the swing leg for 0.9 s and the leg begins to support his weight as the support leg from a 'Heel on' moment when (1) or (3) is satisfied shortly after the start of the landing phase. In addition, Fig. 12 shows the FRF data on both legs and the phase transitions at the start of walking support. The FRF of the heel part is almost zero since participant A

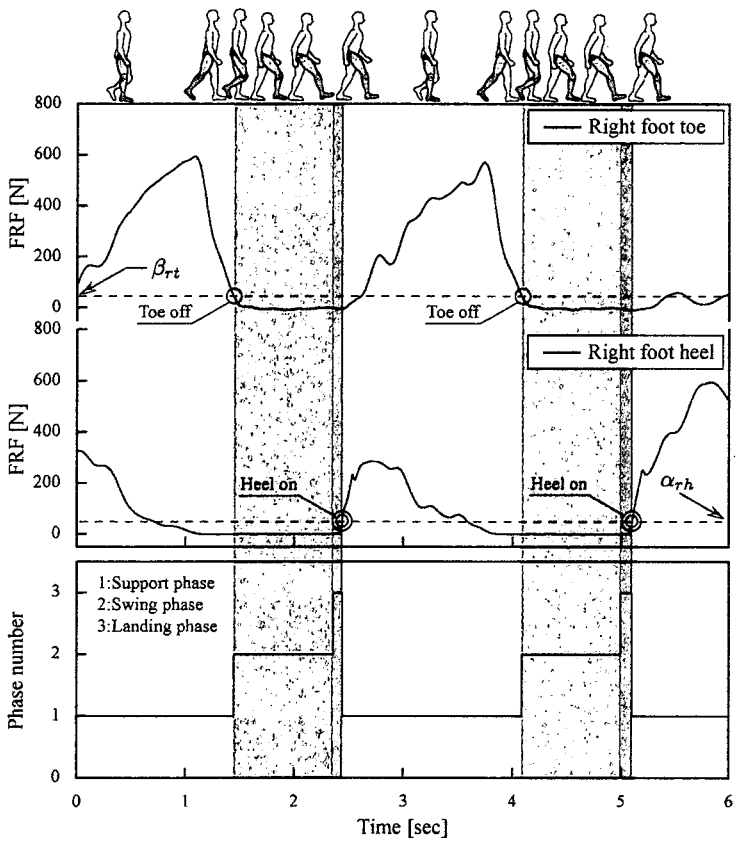

Figure 10. Result of FRF-based intention estimation on the right leg. Data in two steps of the right leg during one walking support for participant A is used. The upper two graphs show the right leg FRF data and the lower one shows right leg phase transition automatically determined through HAL's intention estimator. The right leg performs as the support leg until a 'Toe off' moment (1.4 s) when the FRF on the right toe is below the toe-off threshold β_{rt}, then the leg performs as the swing leg for 0.9 s and finally the leg begins to support his weight as the support leg from a "Heel on" moment (2.4 s) when the FRF on the right heel exceeds the heel-on threshold α_{rh} shortly after the start of the landing phase. Afterwards, the support phase was performed until the next 'Toe off' moment (4.1 s) and the support phase starts from the next 'Heel on' moment (5.1 s) again after the swing and landing phase.

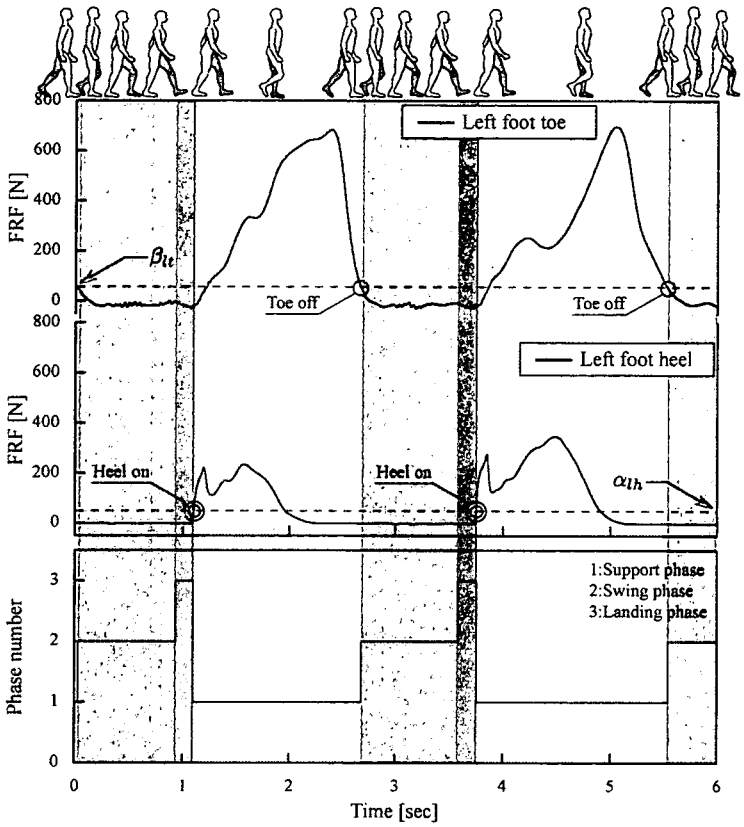

Figure 11. Result of FRF-based intention estimation on the left leg. Data in two steps of the left leg during one walking support for participant A is used. It is the data from the same walking support and in the exact same period as Fig. 10. The upper two graphs show the left leg FRF data and the lower one shows left leg phase transition automatically determined through HAL's intention estimator. The left leg supports his weight as the support leg from a 'Heel on' moment (1.1 s) when the FRF on the left heel exceeds the heel-on threshold α_{lh} until a 'Toe off' moment (2.7 s) when the FRF on the left toe is below the toe-off threshold β_{lt}, then the leg performs as the swing leg for 0.9 s and finally the leg begins to support his weight as the support leg again from the next 'Heel on' moment (3.8 s) shortly after the start of the landing phase. Afterwards, the support has been performed until the next 'Toe off' moment (5.5 s).

leans on the walking frame for the sake of safety. On the other hand, the FRF of the toe part reflects the shift of his COG. At first, he stands on his legs with a load distribution; the right leg supports about 250 N and the left leg supports about 350 N. After that, he shifts his COG in a direction toward his left side, and finally the right and left leg begin to perform as the swing leg and support leg, respectively, when (5) and (6) are satisfied. HAL starts supporting the walk of participant A synchronizing his intentions. Figures 13 and 14 show joint angles, reference and torques of the power units during walking support. Torque data was estimated based on the amount of current provided to each power unit. From the results of joint angles in these

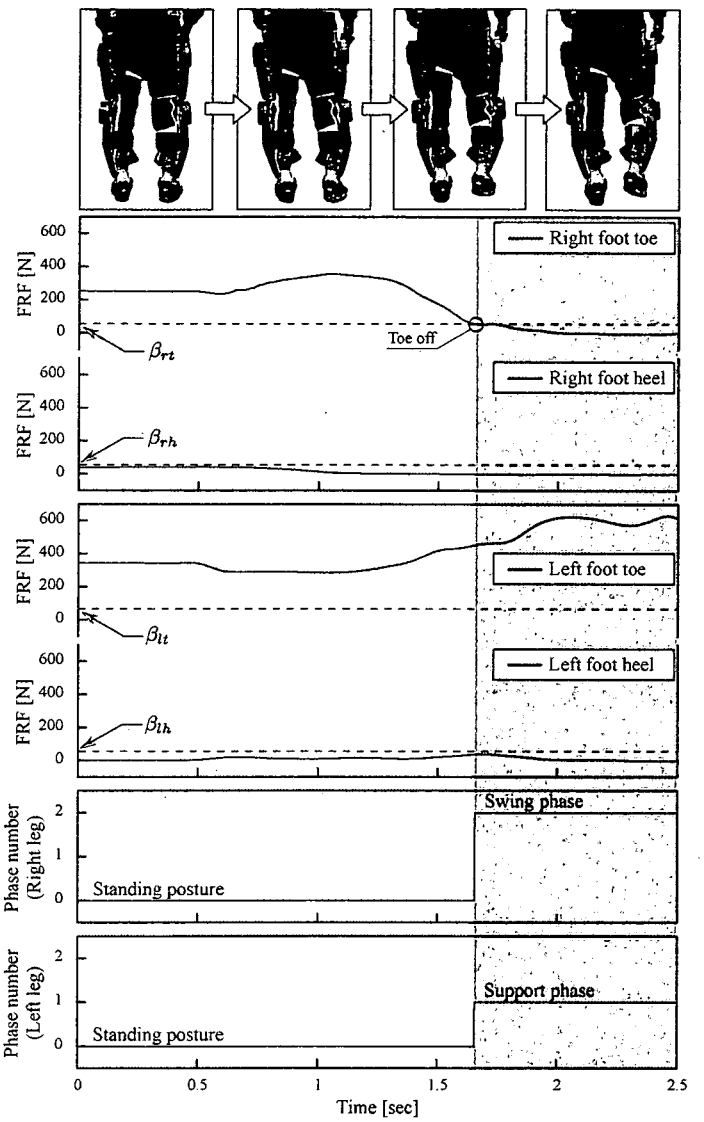

Figure 12. Start of walking support by intention estimation. The upper four pictures show the patient's weight shift onto his left leg for walk initiation. The upper two graphs below the pictures, the middle two graphs and the lower two graphs show the right leg FRF, the left leg FRF, and the right and left leg phase transitions automatically determined through HAL's intention estimator, respectively. The FRFs of both leg heel parts are almost zero since participant A leans on the walking frame, while the FRFs of both leg toe parts reflect his weight shift. At first, he stands on his legs with a load distribution; the right leg supports about 250 N and the left leg supports about 350 N. After that, he shifts his COG in a direction toward his left side, and finally the right and left leg begin to perform as the swing leg and support leg, respectively, when the FRF on the right toe is below the toe-off threshold β_{rt}. HAL starts supporting his walk by synchronizing his intentions.

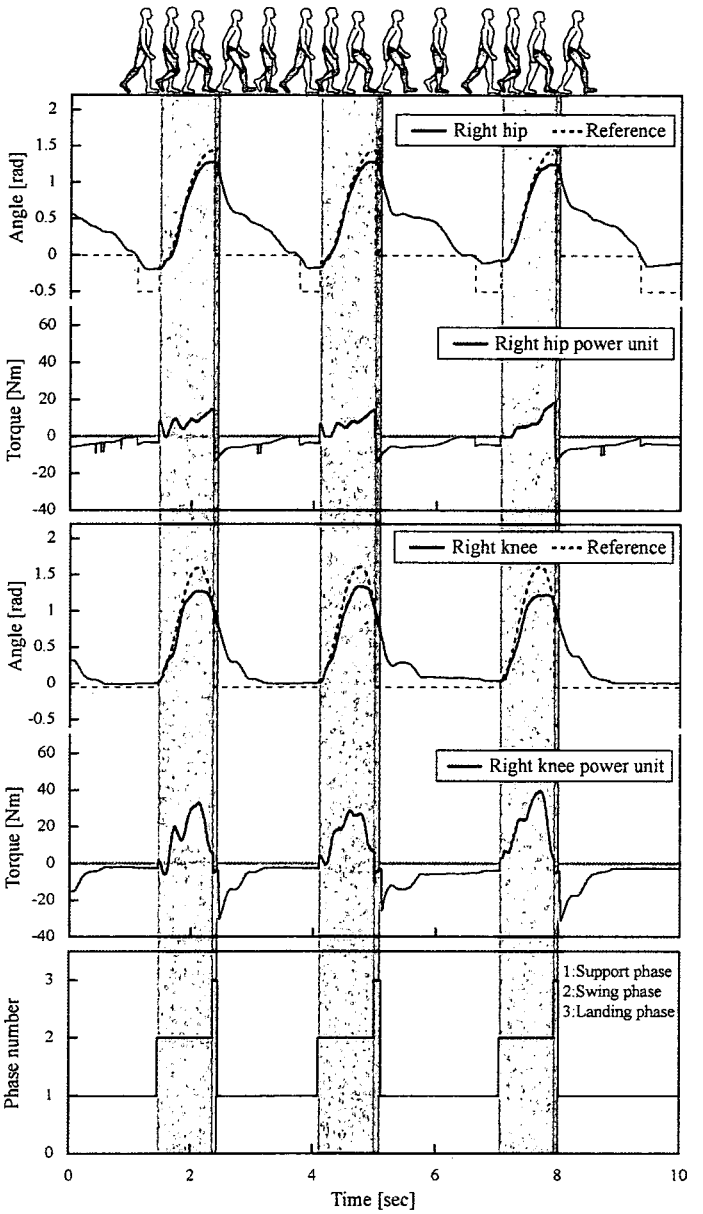

Figure 13. Right leg joint angles with reference angles and power unit torques in each phase. Data in three steps of the right leg during one walking support for participant A is used. His hip and knee joints follow the reference angles based on a healthy person's walk most of one cycle of the supported walk.

figures, his hip and knee joints follow the reference angles most of the time in one cycle of the supported walk. That means HAL supports his walk based on a healthy person's walk as shown in Fig. 7 and he performs a more natural walk with more

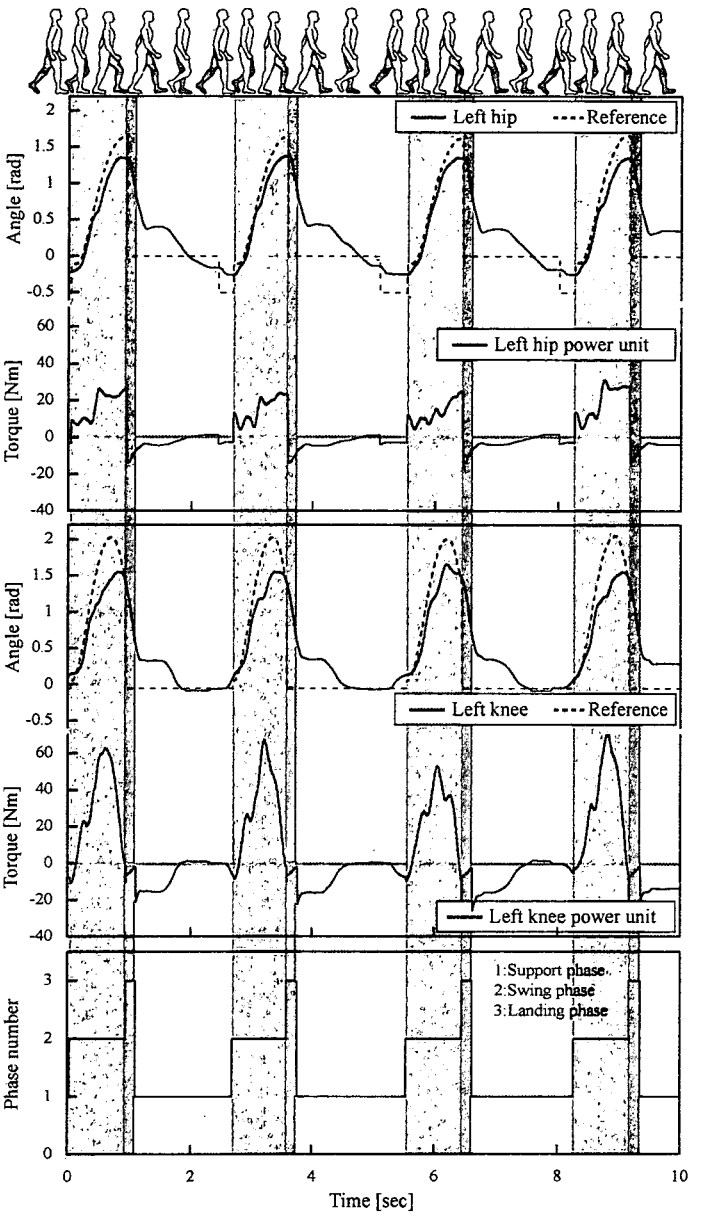

Figure 14. Left leg joint angles with reference angles and power unit torques in each phase. Data in three steps of the left leg during one walking support for participant A is used. It is the data in the same walking support and in the exact same period as Fig. 13. His hip and knee joints follow the reference angles based on a healthy person's walk most of one cycle of the supported walk. Compared to the right leg support shown in Fig. 13, his left hip and knee joints, which have more severe sensory and motor paralysis, require larger torque than his right joints.

step length than his own normal walk. HAL also successfully reduces the risk of his stumbling and falling by assisting his hip and knee flexor muscles during swinging the leg, by lifting up his drop foot, and by assisting his support leg to sustain his weight and prevent sudden knee bends. On the other hand, the results in Figs 13 and 14 show his joints do not follow the references in the latter part of the swing phases, especially the knee joint on his left leg which has more severe sensory and motor paralysis. The knee joint of participant A resists the actuator of HAL since he was used to receiving physical support. The tracking error will be small after enough training for relaxation of the knee joint in the swing phase.

6. CONCLUSIONS

In this paper, we have proposed an algorithm to estimate patients' intentions so that HAL-5 Type-C could support a patient with paraplegia to walk. The estimation algorithm based on the FRF reflecting a wearer's COG control was investigated through the walking support experiments for an incomplete SCI patient with sensory and motor paralysis on both legs. The cycle of reference walking patterns was adjusted for the patient and walking support based on the reference walking was achieved, synchronizing with a patient's intentions estimated by the algorithm. We confirmed that the algorithm successfully estimated a patient's intentions associated with the start and stop of walking, and the beginning to swing a leg based on his weight shift. HAL supported his walk based on a healthy person's walk and he performed more natural walk with more step length than his own normal walk. HAL also reduced the risk of his stumbling and falling by assisting his hip and knee flexor muscles during swinging the leg, by lifting up his drop foot and by assisting his support leg to sustain his weight and prevent sudden knee bends. The proposed walking support can be applied to whoever is able to shift his/her COG by using upper-body functions, including arms and hands, with any support equipment such as a walking frame or a cane. However, it remains to be verified whether the walking support algorithm effectively supports various types of paraplegia patients who have any problems on the lower body through experiments with other physical challenged people. It is one of our future works. In addition, in this walking support, he maintained his balance using a walking frame with his hands as he experienced the support embedded with the proposed intention estimation algorithm for the first time, while he can normally walk with two canes. He can shift his weight during the walking support with the walking frame more easily and smoothly than with his canes. The walking frame could be replaced with his own canes after he gets used to receiving HAL's physical support. In this work, HAL does not stabilize a patient's body posture. Another future work is to develop a stabilizing algorithm and mechanism so that his/her hand regains its own functions.

Acknowledgments

The authors would like to express their sincere gratitude to domestic governments including the Ministry of Education, Culture, Sports, Science and Technology of Japan and foreign governments. Thanks to their warm support, encouragement and advice, we have been making steady progress in our robot suit technology. Moreover, we thank our participants in experiments, and our project members for giving dedicated support and valuable advice with experiments.

REFERENCES

1. J. Okamura, H. Tanaka and Y. Sankai, EMG-based prototype powered assistive system for walking aid, in *Proc. Asian Symp. on Industrial Automation and Robotics*, Bangkok, pp. 229–234 (1999).
2. T. Nakai, S. Lee, H. Kawamoto and Y. Sankai, Development of powered assistive leg for walking aid using EMG and Linux, in: *Proc. Asian Symp. on Industrial Automation and Robotics*, Bangkok, pp. 295–299 (2001).
3. S. Lee and Y. Sankai, Power assist control for walking aid with HAL-3 based on EMG and impedance adjustment around knee joint, in: *Proc. IEEE/RSJ Int. Conf. on Intelligent Robots and Systems*, Lausanne, pp. 1499–1504 (2002).
4. J. E. Pratt, B. T. Krupp, C. J. Morse and S. H. Collins, The RoboKnee: an exoskeleton for enhancing strength and endurance during walking, in: *Proc. IEEE Int. Conf. on Robotics and Automation*, New Orleans, LA, pp. 2430–2435 (2004).
5. T. Nakamura, K. Saito and K. Kosuge, Control of wearable walking support system based on human-model and GRF, in: *Proc. Int. Conf. on Robotics and Automation*, Barcelona, pp. 4405–4410 (2005).
6. H. Kazerooni, R. Steger and L. Huang, Hybrid control of the Berkeley Lower Extremity Exoskeleton (BLEEX), *Int. J. Robotics Res.* **25**, 561–573 (2006).
7. R. Steger, S. H. Kim and H. Kazerooni, Control scheme and networked control architecture for the Berkeley Lower Extremity Exoskeleton (BLEEX), in: *Proc. IEEE Int. Conf. on Robotics and Automation*, Orlando, FL, pp. 3469–3476 (2006).
8. H. Kawamoto and Y. Sankai, Power assist system HAL-3 for gait disorder person, in: *Proc. Int. Conf. on Computers Helping People with Special Needs*, Linz, pp. 196–203 (2002).
9. H. Kawamoto and Y. Sankai, Power assist method based on phase sequence and muscle force condition for HAL, *Adv. Robotics* **19**, 717–734 (2005).
10. M. Sato, H. Ikeuchi, R. Katoh and T. Yamashita, Experimental analysis of reaction force and motion of center of gravity during human gait initiation (characteristics of transferring from transient phase to steady-state phase), *Trans. JSME C* **59**, 3101–3107 (1993). (in Japanese)
11. H. Ikeuchi, K. Shinkoda, R. Katoh, M. Sato and T. Yamashita, Analysis of human transient walking by wavelet transform, in: *Proc. 3rd Int. Symp. on Aritificial Life and Robotics*, Beppu, pp. 695–698 (1998).
12. K. Suzuki, Y. Kawamura, T. Hayashi, T. Sakurai, Y. Hasegawa and Y. Sankai, Intention-based walking support for paraplegia patient, in: *Proc. IEEE Int. Conf. on Systems, Man and Cybernetics*, Waikoloa, HI, pp. 2707–2713 (2005).

APPENDIX

The PD gains of swing leg control k_{rh}, k_{lh}, $\hat{k}_{rh}$, $\hat{k}_{lh}$, k_{rk}, k_{lk}, $\hat{k}_{rk}$ and $\hat{k}_{lk}$ (see (16)) were designed in preliminary experiments. In this Appendix, proportional gains for the hip joints k_{rh} and k_{lh} are expressed by k_{*h}, and proportional gains for the knee joints k_{rk} and k_{lk} are expressed by k_{*k} for convenience. Derivative gains for the hip joints $\hat{k}_{rh}$ and $\hat{k}_{lh}$ are expressed by $\hat{k}_{*h}$, and derivative gains for the knee joints $\hat{k}_{rk}$ and $\hat{k}_{lk}$ are expressed by $\hat{k}_{*k}$.

Figure A1 shows experimental environments, where one leg can swing freely and the other leg supports the participant's weight. At first, the hip or knee joint is controlled by the PD feedback control to examine the frequency response. The reference joint angle patterns are expressed by a sine function with seven different frequencies, ranging from 0.1 to 3.0 Hz, and with 1.0 rad peak-to-peak amplitude. Five different PD gains, with the proportional gain from 20.0 to 200.0 and the derivative gain from 0.02 to 0.20, were tested. Figures A2 and A3 show the frequency responses of hip and knee joints on Bode plots. Then, a unit step response of each joint is examined with six different PD gains. Figures A4 and A5 show the responses of hip and knee joints. From the viewpoint of amplitude characteristics, resonance frequency and phase shift on the hip joint shown in Fig. A2, sufficient response could be obtained when the range that k_{*h} was 100.0–200.0 and $\hat{k}_{*h}$ was 0.10–0.20 at less than 0.5 Hz, which equaled the leg swing frequency in this walking support. In addition, Fig. A4 shows little overshoot and sufficient convergence at the proportional gain of $k_{*h} = 100.0$ and the derivative gain of $\hat{k}_{*h} = 0.10$ for the unit step response. In consideration of those results, we set the hip joint feedback

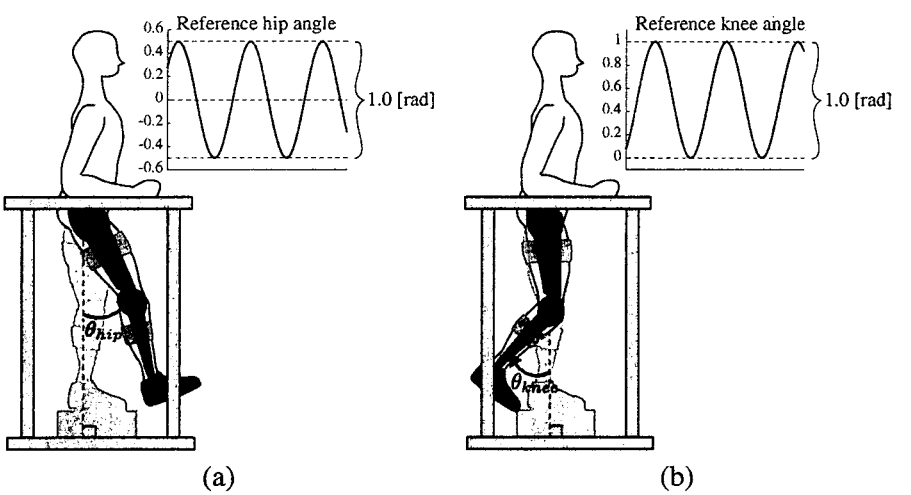

Figure A1. Experimental settings for each joint frequency response. A participant with HAL stands inside a frame with one leg on a raised block so that the other leg can swing freely. The participant is asked to keep the upper body upright and completely relax the leg to follow reference joint motions produced by the power units. Two sine curves show the reference joint angle patterns on each joint. (a) Experimental motion for hip joint. (b) Experimental motion for knee joint.

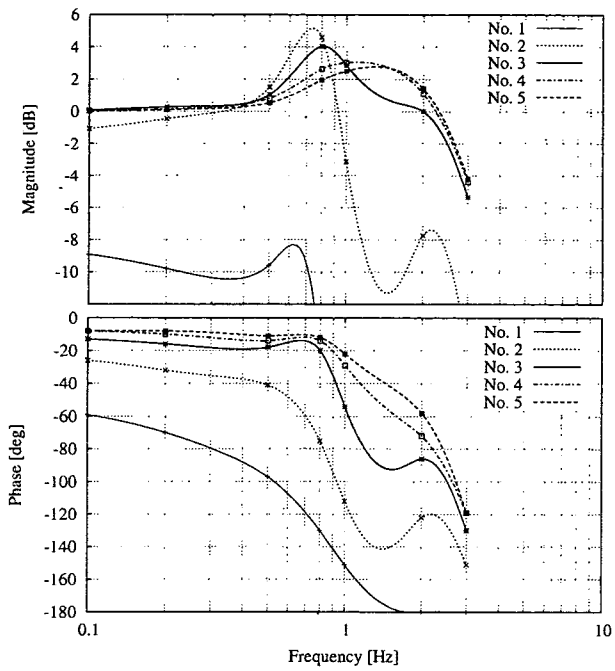

Figure A2. Frequency response of the hip joint shown in a Bode plot. The upper and lower graphs show amplitude and phase characteristics, respectively. Line 1 is a characteristic curve in the case of $k_{*\mathrm{h}} = 20.0$ and $\hat{k}_{*\mathrm{h}} = 0.02$. Similarly, lines 2–5 are for $k_{*\mathrm{h}} = 50.0$ and $\hat{k}_{*\mathrm{h}} = 0.05$, $k_{*\mathrm{h}} = 100.0$ and $\hat{k}_{*\mathrm{h}} = 0.10$, $k_{*\mathrm{h}} = 150.0$ and $\hat{k}_{*\mathrm{h}} = 0.15$, and $k_{*\mathrm{h}} = 200.0$ and $\hat{k}_{*\mathrm{h}} = 0.20$, respectively. All five lines are drawn using a cubic spline curve in order to express the correspondence with seven points in the same set of feedback gains. They, therefore, interpolate the experimental data and would not precisely express the real values.

gains $k_{*\mathrm{h}}$ and $\hat{k}_{*\mathrm{h}}$ to 100.0 and 0.10 in the actual walking support. In the same way, sufficient response was observed when $k_{*\mathrm{k}}$ was 100.0–200.0 and $\hat{k}_{*\mathrm{k}}$ was 0.10–0.20 at less than 1.0 Hz on the knee joint, as shown in Fig. A3. We also set the knee joint feedback gains as 100.0 and 0.10 from the viewpoint of overshoot and oscillation on the step response, as shown in Fig. A5.

ABOUT THE AUTHORS

Kenta Suzuki received the ME degree from the University of Tsukuba, Japan, in 2005. He is currently engaged in the development of HAL and research on Activities of Daily Living support for physically challenged people, and is working toward his PhD at the Graduate School of Systems and Information Engineering, University of Tsukuba. His research interests include biomedical engineering, rehabilitation engineering and 'cybernics'. He received the SICE Young Authors Award from the Society of Instrument and Control Engineers in 2007. He is a member of the IEEE, Robotics Society of Japan, and Society of Instrument and Control Engineers.

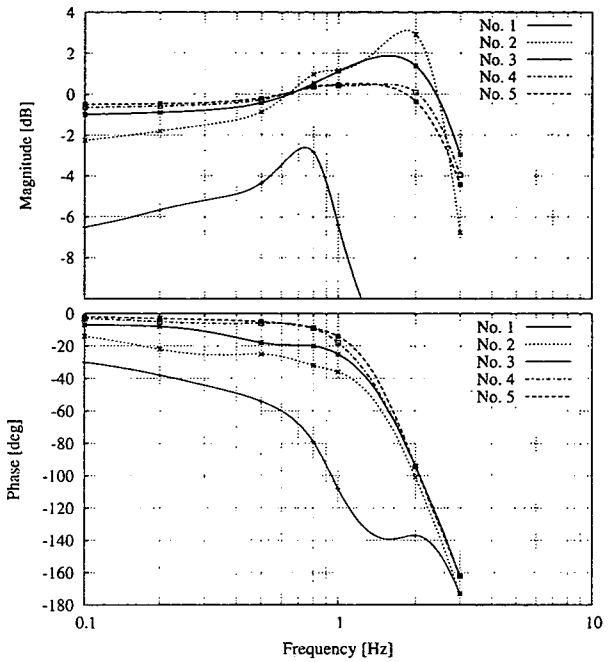

Figure A3. Frequency response of the knee joint shown in a Bode plot. The upper and lower graphs show amplitude and phase characteristics, respectively. Line 1 is a characteristic curve in the case of $k_{*k} = 20.0$ and $\hat{k}_{*k} = 0.02$. Similarly, lines 2–5 are for $k_{*k} = 50.0$ and $\hat{k}_{*k} = 0.05$, $k_{*k} = 100.0$ and $\hat{k}_{*k} = 0.10$, $k_{*k} = 150.0$ and $\hat{k}_{*k} = 0.15$, and $k_{*k} = 200.0$ and $\hat{k}_{*k} = 0.20$, respectively. All five lines are drawn using a cubic spline curve in order to express the correspondence with seven points in the same set of feedback gains. They, therefore, interpolate the experimental data and would not precisely express the real values.

Gouji Mito received the BE and ME degrees from the University of Tsukuba, Japan, in 2004 and 2006, respectively. From 2003 to 2006, he engaged in the project of HAL and contributed to the development of Cybernic Autonomous Control for HAL. He currently works at SECOM Co., Ltd, Japan.

Hiroaki Kawamoto received the ME and PhD degrees from the University of Tsukuba, Japan, in 2000 and 2004, respectively. He was a Research Assistant at the University of Tsukuba Venture Business Laboratory in 2004. Currently, he is a Research Resident at Japan Association for the Advancement of Medical Equipment, mainly engaged in the development of robot suits, and research on enhancement and support of human body functions. His research interests include biomechanics, biorobotics and the human–machine interface, especially human support robots. He received the Best Paper Award from the Robotics Society of Japan in 2006. He is a member of the Robotics Society of Japan and Japan Society of Mechanical Engineers.

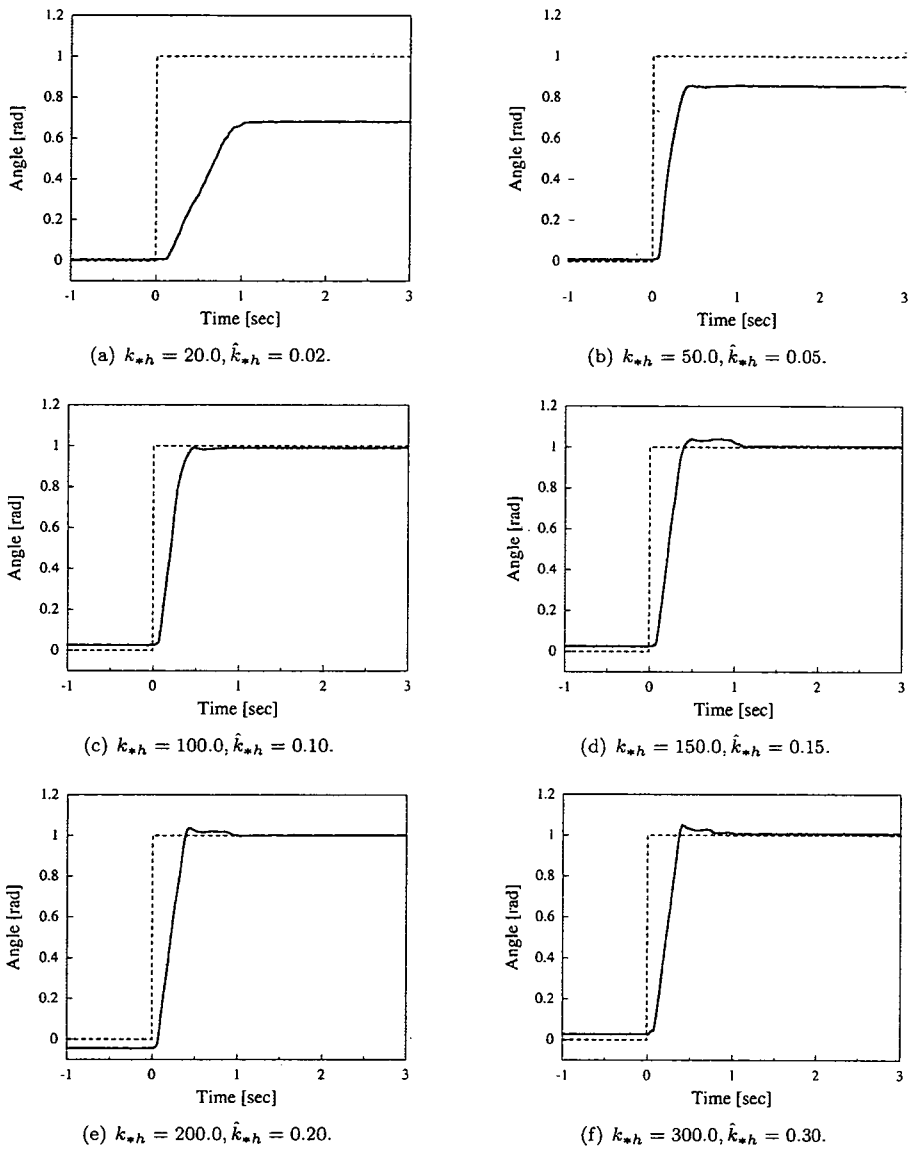

(a) $k_{*h} = 20.0, \hat{k}_{*h} = 0.02$. (b) $k_{*h} = 50.0, \hat{k}_{*h} = 0.05$.

(c) $k_{*h} = 100.0, \hat{k}_{*h} = 0.10$. (d) $k_{*h} = 150.0, \hat{k}_{*h} = 0.15$.

(e) $k_{*h} = 200.0, \hat{k}_{*h} = 0.20$. (f) $k_{*h} = 300.0, \hat{k}_{*h} = 0.30$.

Figure A4. Step responses of the hip joint on six kinds of feedback gains (PD gains). Dashed lines and solid lines in the graphs show step inputs and actual angular variations, respectively.

Yasuhisa Hasegawa received the BE and ME degrees from Nagoya University, Japan, in 1994 and 1996, respectively. From 1996 to 1998, he worked for Mitsubishi Heavy Industries Ltd, Japan. He joined Nagoya University in 1998 and received the Doctor degree from Nagoya University in 2001. He moved to Gifu University in 2003. He is currently an Assistant Professor at the University of Tsukuba, mainly engaged in the research fields of motion assistive systems, dynamic motion control and dexterous robotic hands. He is a member of the IEEE, Japan Society of Mechanical Engineers, Robotics Society of Japan, Society of Instrument and Control Engineers, and Japan Society for Fuzzy Theory and Intelligent Informatics.

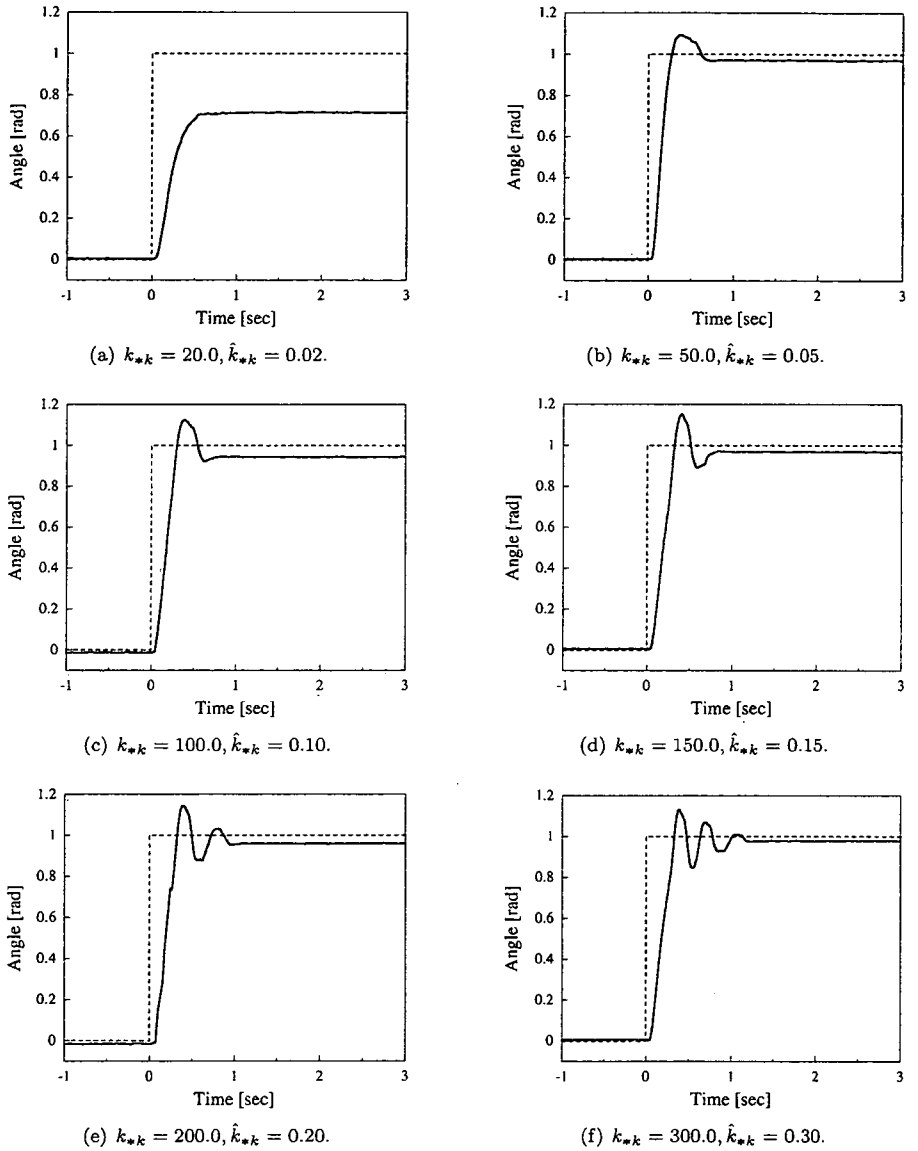

(a) $k_{*k} = 20.0, \hat{k}_{*k} = 0.02$. (b) $k_{*k} = 50.0, \hat{k}_{*k} = 0.05$.

(c) $k_{*k} = 100.0, \hat{k}_{*k} = 0.10$. (d) $k_{*k} = 150.0, \hat{k}_{*k} = 0.15$.

(e) $k_{*k} = 200.0, \hat{k}_{*k} = 0.20$. (f) $k_{*k} = 300.0, \hat{k}_{*k} = 0.30$.

Figure A5. Step responses of the knee joints on six kinds of feedback gains (PD gains). Dashed lines and solid lines in the graphs show step inputs and actual angular variations, respectively.

Yoshiyuki Sankai received the PhD in Engineering from the University of Tsukuba, Japan, in 1987. He was a Japan Society for the Promotion of Science Research Fellow, Assistant Professor, Associate Professor and Professor of Institute of Systems and Engineering in the University of Tsukuba, and a Visiting Professor at Baylor College of Medicine in USA. Currently, he is a Professor of the Graduate School of Systems and Information Engineering in the University of Tsukuba, a Director of UTARC (University of Tsukuba, Division of Advanced Robotics and Cybernics), and a President of CYBERDYNE Inc. He

was/is also a President of the Japan Society of Embolus Detection and Treatment, a Chairman of the International Journal of the Robotics Society of Japan (RSJ), a Member of the Awards Committee of the RSJ, an executive Board Member of the RSJ, and an Executive Editor of *Vascular Lab. Journal.* Now he has become the creator of the world's most advanced robotic technology, HAL, which was introduced by him to the former Prime Minister and his Cabinet members in the Council for Science and Technology Policy at the Prime Minister's office, in 2006. His research interests include the new robotics frontier, 'cybernics': the next generation artificial heart, humanoid control, biomedical science, network medicine, etc. He won the World Technology Award in 2005, Good Design Gold Award in 2006, the 2006 Japan Innovator Award, the Best Paper Award from the Robotics Society of Japan in 2006, Awards from the American Society for Artificial Organs, Award from the International Society for Artificial Organs, etc. Recently, he obtained large Grants from NEDO (Ministry of Economy, Trade and Industry of Japan), large Grants for health science (Ministry of Health, Labor and Welfare of Japan) and a large grant-in-aid scientific research (Ministry of Education, Culture, Sports, Science and Technology of Japan). Now, he is promoting to apply HAL to senior citizens or physically challenged people.